

Binding mode of porphyrins to poly[d(A–T)₂] and poly[d(G–C)₂]

Byeong Hwa Yun ^a, Sun Hee Jeon ^a, Tae-Sub Cho ^a, Seh Yoon Yi ^b,
Ulrica Sehlstedt ^c, Seog K. Kim ^{a,*}

^a Department of Chemistry, College of Sciences, Yeungnam University, Kyongsan City, Kyungbuk 712-749, South Korea

^b Department of Chemistry, Ewha Womans University, Daehyon-Dong, Sodaemun-Ku, Seoul 120-750, South Korea

^c Department of Biophysics, Arrhenius Laboratory, Stockholm University, S 106 91 Stockholm, Sweden

Received 2 December 1996; revised 27 February 1997; accepted 27 February 1997

Abstract

We examined the binding geometry of Co-*meso*-tetrakis (*N*-methyl pyridinium-4-yl)porphyrin, Co-*meso*-tetrakis (*N*-*n*-butyl pyridinium-4-yl)porphyrin and their metal-free ligands to poly[d(A–T)₂] and poly[d(G–C)₂] by optical spectroscopic methods including absorption, circular and linear dichroism spectroscopy, and fluorescence energy transfer technique. Signs of an induced CD spectrum in the Soret band depend only on the nature of the DNA sequence; all porphyrins exhibit negative CD when bound to poly[d(G–C)₂] and positive when bound to poly[d(A–T)₂]. Close analysis of the linear dichroism result reveals that all porphyrins exhibit outside binding when complexed with poly[d(A–T)₂], regardless of the existence of a central metal and side chain. However, in the case of poly[d(G–C)₂], we observed intercalative binding mode for two nonmetalloporphyrins and an outside binding mode for metalloporphyrins. The nature of the outside binding modes of the porphyrins, when complexed with poly[d(A–T)₂] and poly[d(G–C)₂], are quite different. We also demonstrate that an energy transfer from the excited nucleo-bases to porphyrins can occur for metalloporphyrins. © 1998 Elsevier Science B.V.

Keywords: Porphyrins; Polynucleotide; Intercalation; Optical spectroscopy; Fluorescence energy transfer

1. Introduction

Various water-soluble cationic porphyrins and metalloporphyrins form strong complexes with nucleic acids [1,2]. The types of interactions with DNA depend on the nature of the central metal, the structural properties of the porphyrin derivatives and the

ionic strength of the solution. The free bases and square planar complexes such as a porphyrin complex with Ni²⁺ and Cu²⁺, intercalate between the bases of DNA. The porphyrins with axially bound ligands, such as Mn³⁺, Fe³⁺ and Co³⁺, or those with bulky substituents exhibit 'outside binding' because the bulky substituents and the axially bound ligands hinder the intercalative insertion of the porphyrin molecular plane between adjacent base pairs [3]. The charge on the porphyrin core has been

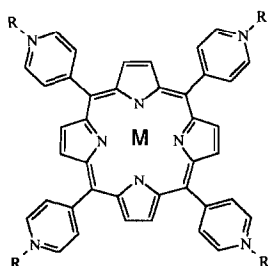
* Corresponding author. Tel.: +82-53-810-2362; fax: +82-53-815-5412; e-mail: skkim@ynuucc.yeungnam.ac.kr

recently shown to affect intercalation vs. outside binding mode [4,5]. Ionic strength-dependent base specificities of porphyrin also have been reported: *meso*-tetrakis(*N*-methylpyridium-4-yl)porphyrin (H_2TMPyP) preferentially binds to the GC-rich region of DNA via intercalation at low ionic strength. While binding to the AT-rich region is more common at higher ionic strength [6–9], H_2TMPyP and its metallo derivatives (Fig. 1) display different affinities for the GC-rich and AT-rich regions of DNA and different types of binding modes when forming complexes with poly[d(A–T)₂] and poly[d(G–C)₂] [3,6–8,10]. The structure of the porphyrin–DNA complex has been extensively studied by various physicochemical methods, including NMR, equilibrium dialysis, viscometric titration and optical spectroscopies [11,12]. These studies support the original proposal that porphyrins intercalate at GC-rich regions and bind in an outside manner at AT-rich sites.

The linear dichroism (LD) technique [13] provides information on the orientations of drugs relative to the DNA helix axis and distinguishes classic intercalation from other binding modes. There are only two reports which address LD measurements on the porphyrin–DNA complex [14,15]. Geacintov et al. [14] studied the conformation of the H_2TMPyP and its zinc(II) derivative complexed with DNA. The dichroism of H_2TMPyP within the Soret band and the Q_y band is consistent with an intercalation conformation in which the plane of the porphyrin ring system is nearly parallel to the DNA helix axis.

However, $ZnTMPyP$ exhibits LD which corresponded to the 62–67° angle between the plane of the porphyrin ring system and the DNA helix. Sehlstedt et al. [15] examined the binding geometries of a series of Co(III) porphyrins and their free ligands to calf thymus DNA by linear and circular dichroism (CD) and a contact energy transfer technique. The nonmetalloporphyrin–DNA complexes were characterized by negative LD corresponding to the 75° angle between the porphyrin ring plane and the DNA helix axis, the negative CD within the Soret band, and a significant contact energy transfer from the DNA bases. In contrast, metalloporphyrins display an orientation angle of around 45°, a positive CD and no contact energy transfer from the DNA bases. These observations support the theory that nonmetalloporphyrins intercalate between the DNA bases whereas metalloporphyrins exhibit an outside binding mode.

The binding geometries of the complexes formed between porphyrins and synthetic polynucleotide such as poly[d(A–T)₂] and poly[d(G–C)₂], have not been reported. In our work, the binding modes of the synthetic porphyrin–polynucleotide complexes formed between two polynucleotides, poly[d(A–T)₂] and poly[d(G–C)₂] and four porphyrins, Co-*meso*-tetrakis(*N*-methylpyridinium-4-yl)porphyrin (CoTMPyP) and Co-*meso*-tetrakis(*N*-butylpyridinium-4-yl)porphyrin (CoTBPYP) and their free ligands (H_2TMPyP and H_2TBPYP) (Fig. 1), were studied by spectroscopic methods including circular and linear dichroism. The purpose of this study is to examine how the binding mode of metallo- and nonmetalloporphyrins with synthetic polynucleotide differ from those of DNA in the low ligand concentration regime (mixing ratio, [ligand] per [DNA base], lower than 0.03), and the effect of the length of the side chains on the binding mode.



M=Co(III)	R=CH ₃	CoTMPyP
M=Co(III)	R=(CH ₂) ₃ CH ₃	CoTBPYP
M=2H	R=CH ₃	H ₂ TMPyP
M=2H	R=(CH ₂) ₃ CH ₃	H ₂ TBPYP

Fig. 1. Molecular structure of porphyrins.

2. Materials and methods

2.1. Materials

Poly[d(A–T)₂] and poly[d(G–C)₂] was purchased from Pharmacia and dissolved in 5 mM cacodylic buffer containing 1 mM EDTA and 100 mM NaCl at

pH 7.0 by exhaustive stirring at 4°C. The polynucleotide solution was dialyzed against a 20 mM NaCl and 5 mM cacodylic buffer at 4°C. This buffer was changed several times at 5-h interval and was used throughout this work. The concentrations of porphyrins and polynucleotides were determined spectrophotometrically [15].

All spectroscopic measurements were performed for porphyrin–polynucleotide complexes with a mixing ratio, R , of 0.005, 0.01, 0.015, 0.02, 0.025 and 0.03 of [ligand] per [DNA base]. The polynucleotide concentration was 200 μM in the nucleotide base. The resulting spectroscopic properties for the samples using the above ratios were essentially the same, indicating that the binding properties are independent of the mixing ratios employed. The results shown in this work are those for the highest mixing ratio in each case. The samples which were used for absorption, circular and linear dichroism measurements were diluted 20 times for the energy-transfer measurements to avoid inner filter effect.

2.2. Linear dichroism

Linear dichroism on flow-aligned DNA was measured in a Wada-type couette cell [16] on a Jasco J500A spectropolarimeter, as described earlier [13,17–20]. The path length was 1.0 mm. The reduced linear dichroism (LDr)—the ratio between the measured LD and isotropic absorbance $A_{\text{iso}}(\lambda)$ at a given wavelength λ —is related to the angle α , between the light-absorbing transition dipole moment and the local helix axis of DNA:

$$\text{LDr}(\lambda) = \frac{\text{LD}(\lambda)}{A_{\text{iso}}(\lambda)} = \frac{3S(3\langle\cos^2\alpha\rangle - 1)}{2} \quad (1)$$

where S is an orientation function: $S = 1$ for DNA perfectly aligned, parallel to the flow lines and $S = 0$ for isotropic orientation. The brackets denote the ensemble average over the angular distribution [19]. By assuming no overlap of DNA and the porphyrin transition, and an effective angle of 86° between the $\pi \rightarrow \pi^*$ transition moments of the nucleotide bases and the polynucleotide helix axis, the orientation factor S may be determined from the polynucleotide dichroism at 260 nm. This assumption is valid only

when the ligand concentration is much lower than DNA, which is our case where the highest mixing ratio ([porphyrin] per [DNA base]) is 0.03. In the present case, as a result of the degenerate in-plane polarization of $\pi \rightarrow \pi^*$ transitions of the porphyrin chromophore, the apparent α value corresponding to a tilt of the porphyrin plane by the angle β , will be larger than the tilt (i.e., $\alpha > \beta$). The tilt is obtained by replacing $2\cos^2\alpha$ in Eq. (1) by $\cos^2\beta$ [21]. From the determined S value, we calculated an effective value of the β , which is the angle of the porphyrin transition moment (in-plane polarized $\pi \rightarrow \pi^*$ transitions in the Soret band) relative to the polynucleotide helix axis. Large β values (80–90°) indicate intercalation whereas small values, such as 40–50°, are consistent with groove binding and exclude the intercalative binding mode.

2.3. Absorption and CD spectra

Absorption spectroscopy is the most convenient tool for examining the interaction between drugs and DNA. The binding of a drug to DNA results, in general, in a broadening and red-shift and hypochromism in the drug absorption band. The absorption spectra were run on a Jasco V-550 or Hewlett Packard 8452A diode array spectrophotometer.

The circular dichroism, defined by the difference between the absorbance measured with left- and right-hand circularly polarized lights, may provide information on two levels regarding the drug–polynucleotide complex. First, polynucleotide conformation can be studied through the CD of intrinsic polynucleotide absorption near 260 nm. Second, it is possible to extract some information on the conformation of porphyrins from the induced CD (ICD) of a DNA-bound porphyrin. Although the origin of ICD of the porphyrin–DNA complex is not clear, it is believed to be induced by the interaction between the transition moments of achiral porphyrin and chirally arranged DNA base transitions or by excitonic interaction of the DNA-bound porphyrin [22]. All CD spectra were measured on a Jasco J-500C spectropolarimeter which displayed the CD in millidegrees ellipticity. Path lengths for both absorption and CD measurements were 1.0 cm.

2.4. Contact energy transfer

The method to evaluate the amount of energy transferred from DNA bases to the bound ethidium (the contact energy transfer) is explained in detail by Le Pecq and Paoletti [23]. This technique is occasionally used to examine if the drug is in contact with DNA bases [15,24–26]. It was recently observed that the excited energy of the nucleobases can be transferred not only to the intercalators but also to the minor groove binders, such as 4',6-di-amidino-2-phenylindole or Hoechst 33258 [27]. The amount of energy transfer is denoted by the ratio

$$Q(\lambda) = \frac{Q_b(\lambda)}{Q_f(\lambda)} \quad (2)$$

where $Q_b(\lambda)$ and $Q_f(\lambda)$ are the quantum efficiencies of the bound and free ethidium. This ratio is calculated for each wavelength using the expression

$$Q(\lambda) = \frac{I_b(\lambda) \varepsilon_f(\lambda)}{I_f(\lambda) \varepsilon_b(\lambda)} \quad (3)$$

where I and ε are the measured fluorescence intensities and molar extinction coefficients at wavelength λ , and b and f refer to the bound and free ligands. The ratio $Q(\lambda)/Q_{320\text{ nm}}$ was then plotted with respect to the wavelength. The normalization factor $Q_{320\text{ nm}}$ was chosen because the absorbance of polynucleotide at this wavelength is negligible. The fluorescence excitation spectrum at 220 nm–320 nm was recorded through the emission window at 660 nm with a slit width of 40 nm. The excitation slit width was 4 nm. The spectra are averaged over an appropriate number of scans to enhance the signal to noise ratio. A conventional Perkin Elmer LS50B fluorometer and Jasco V-550 UV-VIS spectrophotometer were used to detect the absorption and fluorescence signal. A cut-off filter was used at the emission window to avoid double frequency radiation.

3. Results

A number of observations were made from our comparative study of a set of porphyrins and poly[d(A–T)₂] and poly[d(G–C)₂]. The porphyrins

were chosen to include H₂TMPyP and H₂TBPyP, which have no axial ligands, and CoTMPyP and CoTBPyP which have diaxial ligand. The diaxial ligands are expected to prevent the intercalation of porphyrin into polynucleotide bases. The porphyrins possessing side chains of a different length (methyl and butyl groups on the *para* position of pyridinium rings) were also compared. Poly[d(A–T)₂] and poly[d(G–C)₂] are used as a model for AT- and GC-rich DNA.

3.1. Absorption spectra

The binding of certain drugs to DNA produces hypochromism broadening of the envelope and a red-shift in the drug absorption band. These effects are particularly pronounced for intercalators. The absorption spectra in the Soret band of porphyrins in the presence and absence of poly[d(A–T)₂] and poly[d(G–C)₂] are depicted in Fig. 2 in which corresponding polynucleotide absorption spectrum has been subtracted from those of the mixtures. The change in the absorption pattern in the DNA absorption region upon mixing of porphyrin and DNA may reflect the change in the DNA conformation or interaction between porphyrin and nucleobases. At this point, these reasons for which the absorbance change in this region cannot specifically distinguish, we will discuss only the changes in the absorption spectrum in the Soret band. The absorption spectra of CoTMPyP and CoTBPyP when complexed with poly[d(G–C)₂] are almost identical to those of polynucleotide-free CoTMPyP and CoTBPyP (Fig. 2a and b), except that in the case of CoTBPyP, 4 nm red-shift is observed. When bound to poly[d(A–T)₂], both CoTMPyP and CoTBPyP exhibited a 20–30% hyperchromism and a 5 nm red-shift. In the case of the nonmetalloporphyrin (Fig. 2c and d), the changes in the absorption spectrum are quite different from those of the metalloporphyrins. In the presence of poly[d(A–T)₂], both H₂TMPyP and H₂TBPyP exhibited a red-shift (9 nm) and a small hypochromism (2–9%). When these drugs are bound to poly[d(GC)₂], a 41–42% hypochromism and a 22–23 nm red-shift are observed. Changes in the absorption spectrum in the Soret band depend upon the presence of central Co(III) atom, but the length of the alkyl

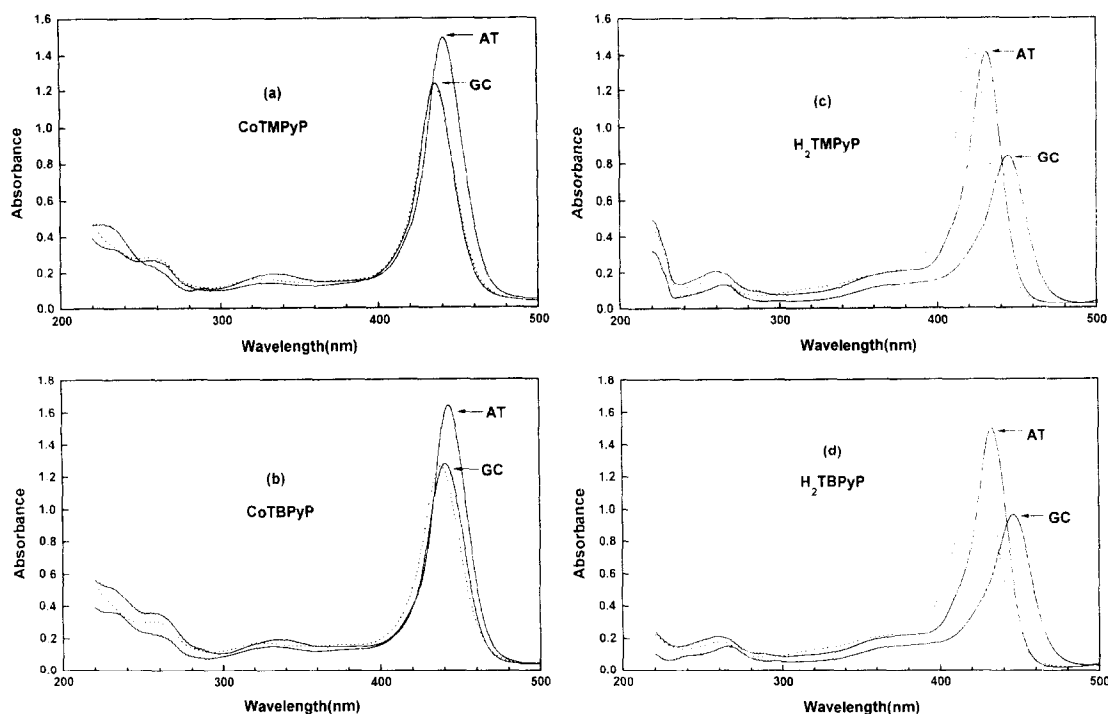


Fig. 2. Absorption spectra of (a) CoTMPyP, (b) CoTBPYP, (c) H₂TMPyP and (d) H₂TBPYP in the presence of poly[d(A-T)₂] and poly[d(G-C)₂] and those in the absence of polynucleotide (dotted curve). The data were collected for 200 μ M polynucleotide and $R = 0.005, 0.010, 0.015, 0.020, 0.025$ and 0.030 . The absorption spectrum of corresponding polynucleotide was subtracted from that of the mixture. Only those for the highest mixing ratio and free porphyrins are shown. The shape of absorption spectra are invariant among the mixing ratios when normalized to concentration.

side chain at pyridine residue does not alter the absorption change. These changes in the absorption spectra were similar to those reported for DNA [15].

3.2. Induced CD

The porphyrins and metalloporphyrin derivatives used here do not yield CD spectra in the absence of polynucleotide, but CD spectra were induced for various porphyrins in the presence of DNA, due to the interaction between the transition moments of the achiral porphyrin and chirally arranged DNA base transitions. Representative ICD spectra for porphyrins complexed with poly[d(A-T)₂] and poly[d(G-C)₂] are shown in Fig. 3. All the examined porphyrins display positive ICD spectra in the Soret band and a strong negative band around the 280-nm region when bound to poly[d(A-T)₂] (Fig. 3a). The ICD spectra of nonmetalloporphyrins bound to poly[d(G-C)₂] display a quite different behavior (Fig. 3b). In the Soret band all porphyrins exhibit a nega-

tive ICD band. Around 270–290 nm, we observed a negative band for the nonmetalloporphyrin–poly[d(G-C)₂] complex and a positive one for the CoTMPyP–poly[d(G-C)₂] and CoTBPYP–poly[d(G-C)₂] complexes. These observations suggest that the sign of the ICD spectrum in the Soret band region depends upon the nature of the nucleobases, but that in the 270 nm–290 nm region, it depends upon the binding mode (see Sections 4.1 and 4.2). The changes in the CD spectrum in the polynucleotide absorption region reflect either the exciton interaction of nucleobases with bound porphyrin or the conformation change of polynucleotide upon porphyrin binding. Since this origin cannot be distinguished at this point, the CD signal in this region will not be discussed further.

3.3. LD and LDr

LD and LDr spectra of porphyrins complexed with poly[d(A-T)₂] and poly[d(G-C)₂] are depicted

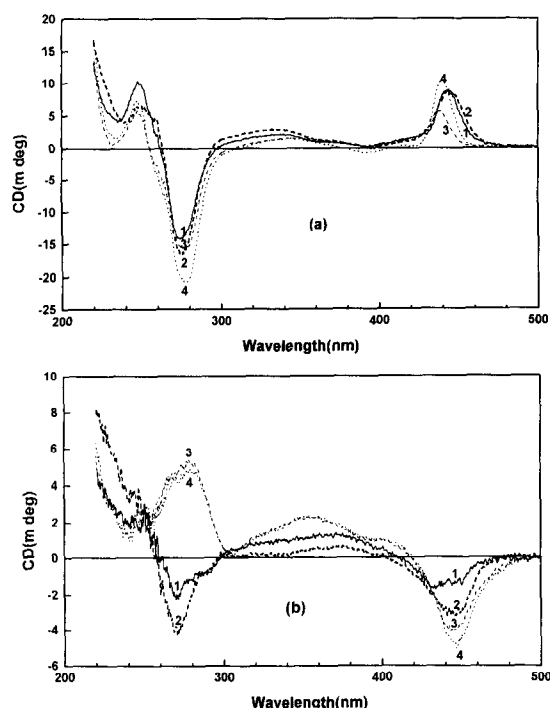


Fig. 3. CD spectra of porphyrins bound to (a) poly[d(A-T)₂] and (b) poly[d(G-C)₂] with [polynucleotide] = 200 μ M, [porphyrin] = 6 μ M. Corresponding polynucleotide spectrum was subtracted. Curve assignment: 1, CoTMPyP; 2, CoTBPpP; 3, H₂TMPyP; and 4, H₂TBPpP.

in Figs. 4 and 5. When bound to poly[d(A-T)₂], all porphyrins show a negative band within the Soret band, regardless of the presence of a central Co(III) metal. In contrast, when complexed with poly[d(G-C)₂], H₂TMPyP and H₂TBPpP exhibit a negative LD signal and, in the case of metalloporphyrin, both a very small negative (near zero) LD for CoTBPpP and a bisignate LD signal for CoTMPyP are apparent in this region. These observations suggest that the binding geometry of the metalloporphyrin, which is known to bind outside of DNA [15], is very different on poly[d(A-T)₂] and on poly[d(G-C)₂]. Negative LD signals in the drug absorption band are usually considered to be an indication that the transition moments, which are oriented within the planes of the drug molecules, are tilted more perpendicularly than in parallel to the flow lines [16,17]. However, in the porphyrin–polynucleotide complex case, it is considered as an effect of the degeneracy or near-degeneracy

of electronic states in the effective four-fold symmetry of metalloporphyrins [15].

The LDr for all complexes is negative for the polynucleotide in the $\pi \rightarrow \pi^*$ transition region around 260 nm, which agrees with the polynucleotide base planes for the polynucleotides being nearly perpendicular to the helix axis (Fig. 5a and b). The significant decreases in the LDr magnitude in this region (25–50% decreases for a base:porphyrin ratio of 33), apparent for all porphyrin–poly[d(A-T)₂] complexes (Fig. 5a) and CoTMPyP–poly[d(G-C)₂] and CoTBPpP–poly[d(G-C)₂] complexes (Fig. 5b), suggest decreases in the orienting ability of the polynucleotides; binding of any porphyrin to poly[d(A-T)₂] and binding of metalloporphyrin to poly[d(G-C)₂] either create regions of higher flexibility or causes bends or kinks at the binding sites of the polynucleotides. In contrast, binding of

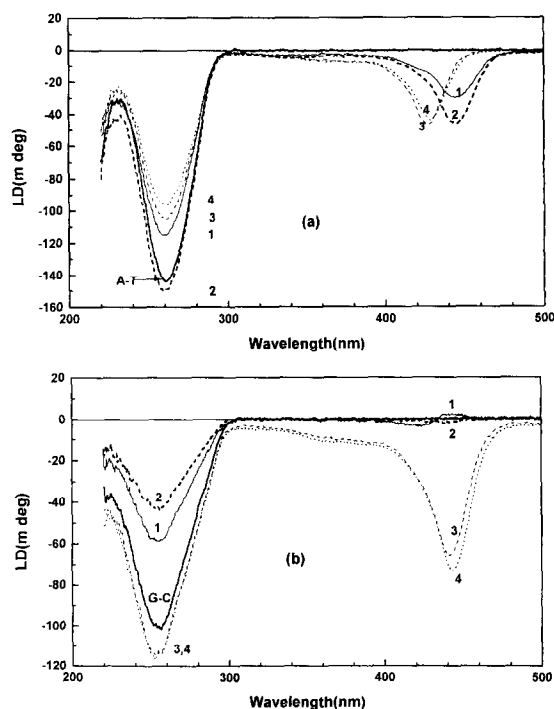


Fig. 4. The LD of various porphyrins bound to (a) poly[d(A-T)₂] and (b) poly[d(GC)₂] with [polynucleotide] = 200 μ M, [porphyrin] = 6 μ M. Curve assignment: 1, CoTMPyP; 2, CoTBPpP; 3, H₂TMPyP; and 4, H₂TBPpP. LD of porphyrin-free polynucleotides are presented as thick solid curves.

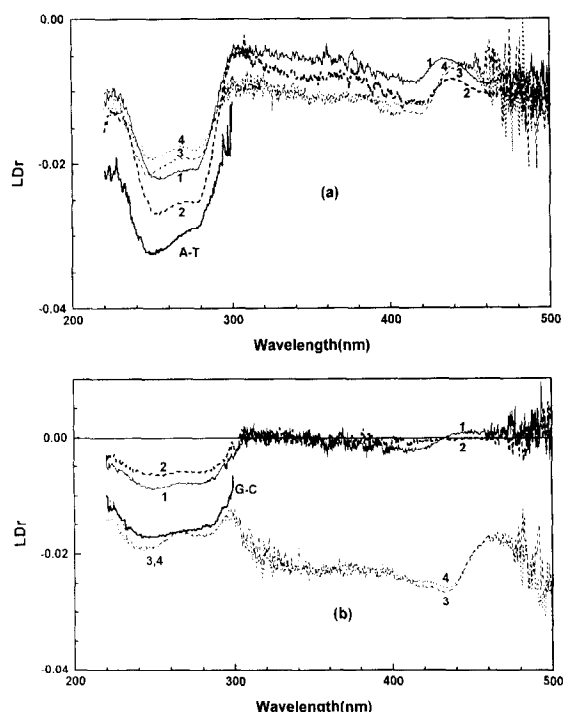


Fig. 5. The LDr spectra of various porphyrins bound to (a) poly[d(A-T)₂] and (b) poly[d(G-C)₂]. The conditions and the curve assignments are the same as in Fig. 4.

H₂TMPyP and H₂TBPyP to poly[d(G-C)₂] causes a slight increase of the LDr magnitude in the polynucleotide absorption region which is consistent with an intercalative binding mode [15]. Increase in the LDr magnitude may be due to the DNA stiffening upon ligand intercalation.

The true tilt angle, β , between the in-plane transition moments of porphyrin and the polynucleotide helix axis was obtained by replacing $\cos^2\beta$ with $2\cos^2\alpha$ in Eq. (1) [21]. The angle β for the porphyrin–poly[d(A-T)₂] complex in the Soret maximum is in the range of 45–50°; the range is 30–40° for the metalloporphyrins–poly[d(G-C)₂] complexes. Although the LDr values for the porphyrin–poly[d(A-T)₂] complexes are consistent with the angle that the grooves made with the polynucleotide helix, the variations in the LDr values in the metalloporphyrins–poly[d(G-C)₂] complexes differentiate it from well-known minor groove binders such as

4',6-diamidino-2-phenylindole [28–30] and Hoechst 33258 [30,31]. In contrast, the LDr magnitudes within the Soret band are comparable to those of the polynucleotide absorption regions for the H₂TMPyP–poly[d(G-C)₂] and H₂TBPyP–poly[d(G-C)₂] complexes (Fig. 5b). This type of LDr is typical for a drug which is intercalated between the polynucleotide bases [15]. The wavelength-dependent LDr in the Soret band suggests that the nonmetalloporphyrins are tilted in the intercalation pocket of poly[d(G-C)₂].

3.4. Contact energy transfer

The fluorescence quantum yields of drugs contacting polynucleotide bases are increased for excitation around 260 nm. This increase corresponds to an energy transfer from polynucleotide bases to the bound drugs. Energy transfer from DNA bases to bound drugs has been used as an indication that the drug is intercalated between the nucleobases [15,23–26]. However, recent study shows that minor groove-bound drugs exhibit the similar $Q(\lambda)/Q_{320\text{nm}}$ plot, indicating that the excited energy of the nucleobases can be transferred not only to intercalated drug but also to minor groove-bound ones [27]. The energy transfer therefore, indicates that the drug is in contact with the nucleobases rather than intercalated. Results from an energy transfer measurement for porphyrins bound to poly[d(G-C)₂] and

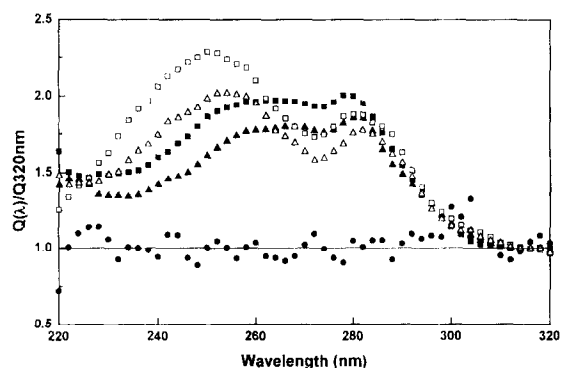


Fig. 6. The ratio $Q(\lambda)/Q_{320\text{nm}}$ for porphyrin bound to poly[d(A-T)₂] (closed symbols) and poly[d(G-C)₂] (open symbols). The ratio for H₂TMPyP is marked by squares and for H₂TBPyP by triangles. The metalloporphyrins do not exhibit any energy transfer, one is indicated for the CoTMPyP–poly[d(G-C)₂] complex by closed circles.

poly[d(A–T)₂] are depicted in Fig. 6. The energy transfer occurs only for the nonmetalloporphyrin complexed with poly[d(A–T)₂] and poly[d(G–C)₂]. The metalloporphyrins–poly[d(A–T)₂] complexes, as well as those complexed with poly[d(G–C)₂], does not exhibit the energy transfer. These observations indicate that nonmetalloporphyrins are in contact with polynucleotide bases, regardless of their binding modes but metalloporphyrins are not. The shape of the $Q(\lambda)/Q_{320\text{ nm}}$ plot is similar to those observed for the nonmetalloporphyrin–DNA complexes [15]. The size of the side chains (methyl and butyl groups) on the *para* position of pyridinium rings did not seem to affect the shape of the $Q(\lambda)/Q_{320\text{ nm}}$ plot.

4. Discussion

4.1. Binding mode of porphyrins to poly[d(A–T)₂]

The LD spectroscopic characteristics of the porphyrins bound to poly[d(A–T)₂] are similar regardless of the presence of the central Co(III) ion, suggesting that the conformations of metallo- and nonmetalloporphyrins are similar when complexed with poly[d(A–T)₂]. Side chains with different lengths do not alter the conformation. The angles of the electric transition moment in the Soret band, which correspond to *x* and *y* in the plane transition, are 45–50° (relative to the polynucleotide helix axis), which coincides with the angle of the groove with respect to polynucleotide helix axis. This angle rules out the possibility of an intercalative binding mode for porphyrin as well as a random outside binding mode, in which positively charged porphyrin bind to a negatively charged phosphate group by electrostatic interaction. In the former case, the angle between the porphyrin molecular plane and the polynucleotide helix axis would be near perpendicular: in the latter case the LDr magnitude is expected to be zero because the orientation of the porphyrin chromophore in this binding mode is random. Therefore, the orientation of the chromophore was consistent with groove binding. The exact location of porphyrin in the polynucleotide, either in the major groove or minor groove, cannot be distinguished by LD measurements. Decreases in the LDr magnitude in the polynucleotide absorption region indicate that the

flexibility of polynucleotide is increased (orientation is difficult) upon porphyrin binding, suggesting that porphyrin is bound in the partially melted region of polynucleotide.

Although the ICD spectrum of polynucleotide-bound drugs is known to be sensitive to the binding geometry of the drug, the presence of a central metal and a change in the side chain length did not alter the ICD spectrum of the complex when bound to poly[d(A–T)₂], demonstrating that the binding geometry of porphyrin is not affected by the presence of the central Co(III) ion and the length of the side chain. The ICD spectrum was mixing ratio-independent under our condition, indicating that the conformation of porphyrin is invariant with our low mixing ratio, despite the possibility that some outside binding porphyrin could be self-stacked at a high mixing ratio [22].

In contrast to the strong energy transfer from nucleobases to the bound porphyrin observed for the nonmetalloporphyrin–poly[d(A–T)₂] complex, the excited energy of the nucleobases was not transferred to porphyrins when Co(III) was present. Two factors, distance and relative orientation, may affect the efficiency of the energy transfer. Since the orientations of the porphyrin in the presence and absence of the central metal was similar when bound to poly[d(A–T)₂], the difference in the fluorescence energy transfer may be attributed to the distance between the porphyrin and nucleobases. The central octahedral metal complex may inhibit the deep insertion of porphyrin from the groove. The distance between the nucleobases and porphyrin is so great, compared to nonmetalloporphyrin that the energy transfer cannot occur while the binding geometry is remained to be the same. From these observations, we concluded that when bound to poly[d(A–T)₂], metalloporphyrin is likely to be at the mouth of the groove, at which part of the molecular plane is inserted into the groove, while nonmetalloporphyrin is deep in the groove to contact or near contact with the nucleobases.

4.2. Binding mode of the porphyrins to poly[d(G–C)₂] complex

The shape of the LDr of the nonmetallo–poly[d(G–C)₂] and metalloporphyrin–poly[d(G–C)₂]

complexes are quite different, indicating that the binding geometries of these two classes of porphyrin are different. When the central metal is absent, the LDr of the complex exhibits a typical intercalation binding mode (characterized by increases in the magnitude in the polynucleotide absorption region (around 260 nm) upon porphyrin binding), and the magnitude in the Soret band is comparable to that in the polynucleotide absorption region. The increases in the LDr magnitude in the polynucleotide absorption region indicate that the orienting ability of the complex is increased. Intercalation of a drug between the nucleo-bases typically results in the unwinding and elongation of polynucleotide, which increases the orienting ability. The observed increases in the LDr magnitude in the polynucleotide absorption region are, therefore, consistent with the intercalation of nonmetalloporphyrin to poly[d(GC)₂]. The LDr magnitude in the Soret band is as large as in the polynucleotide absorption region, indicating that the molecular plane of porphyrin is parallel to that of nucleo-bases (perpendicular to the helix axis), which is a strong indication for the intercalation. The metalloporphyrins–poly[d(G–C)₂] complexes exhibited 30–40° angle between the molecular plane of the porphyrin and the polynucleotide helix axis, with a decreasing LDr magnitude in the DNA absorption region. This 30–40° angle is somewhat small (the molecular plane of porphyrin is more parallel to nucleo-bases), compared to the angle that the minor groove makes with the helix axis. The minor groove of the polynucleotide is narrow and deep, resulting in little freedom for the bound drugs. For this reason, the angle between the transition moment of the drug and the helix axis is near 45° for most minor groove-binding drugs. Considering the steric effect of the central metal atom, it is conceivable that metalloporphyrins bind either at the mouth of the minor groove or in the major groove. Considering (1) the 30–40° angle which is somewhat smaller than the angle that the minor groove makes with the helix axis, and (2) the presence of the exocyclic amino group in the minor groove of poly[d(G–C)₂], which provides the steric hindrance for the minor groove binding drugs [29], we propose that porphyrins may be located in the major groove of poly[d(G–C)₂].

The ICD spectra of metallo- and nonmetalloporphyrin, when complexed with poly[d(G–C)₂], are

similar in the Soret band, but the sign was the opposite of that in the DNA absorption region. Two origins for a CD spectrum below 300 nm are possible: changes in the polynucleotide conformation upon binding of drug and/or the induced CD of porphyrin due to interaction between the transition moment of bound porphyrin and the polynucleotide base transitions, as we noted in Section 3.2. These cannot presently be distinguished, and therefore further analysis of CD in this region was ceased.

Similar to the poly[d(A–T)₂] case, the metalloporphyrin–poly[d(G–C)₂] complexes exhibit a null energy transfer, indicating that the metalloporphyrin molecule is quite distant from the nucleo-bases. It is not surprising that a strong energy transfer occurs for the intercalated porphyrin because, by definition, porphyrin is in contact with the nucleo-bases.

5. Conclusions

Based on our CD, LD and contact energy transfer measurements on H₂TMPyP, H₂TBPyP, CoTMPyP and CoTBPyP, we concluded that: (1) The length of the side chain does not affect the binding geometry of porphyrin. (2) The excited energy can be transferred from the nucleo-bases even to the porphyrin, which is known to bind to the ‘outside’ of the polynucleotide. (3) Nonmetalloporphyrins are confirmed to be intercalated to poly[d(G–C)₂], while they bind to the groove of the poly[d(A–T)₂]. (4) The binding geometries of metalloporphyrins are different when complexed with poly[d(A–T)₂] and poly[d(G–C)₂], although both can be considered as groove binding.

Acknowledgements

This work was supported by the Basic Research Institute Program, Ministry of Education, South Korea (Grant No. BSRI-96-3436) and the Internal Research Grant of Yeungnam University. The authors are indebted to Bengt Nordén of Chalmers University of Technology for allowing us to use linear dichroism spectroscopy and for the helpful discussions.

References

- [1] R.F. Pasternack, E.J. Gibbs, in: T. Tullius (Ed.), *Metal–DNA Chemistry*, American Chemical Society, Washington, DC, 1989, pp. 59–73.
- [2] R.J. Fiel, J. Biomol. Struct. Dyn. 6 (1989) 1259.
- [3] R.F. Pasternack, E.J. Gibbs, J.J. Villafranca, *Biochemistry* 22 (1983) 2406.
- [4] R. Kuroda, E. Takahashi, C.A. Austin, L.M. Fisher, *FEBS Lett.* 262 (1990) 293.
- [5] L.G. Marzilli, G. Petho, M. Lin, M.S. Kim, D.W. Dixon, *J. Am. Chem. Soc.* 114 (1992) 7575.
- [6] M.J. Carvlin, R.J. Fiel, *Nucleic Acids Res.* 11 (1983) 6121.
- [7] M.J. Carvlin, E. Mark, R.J. Fiel, *Nucleic Acids Res.* 11 (1983) 6141.
- [8] R.F. Pasternack, A. Antebi, B. Ehrlich, D. Sidney, E.J. Gibbs, S.L. Bassner, L.M. Depoy, *J. Mol. Catal.* 23 (1984) 235.
- [9] R.F. Pasternack, P. Garrity, B. Ehrlich, C.B. Davis, E.J. Gibbs, G. Orloff, A. Giartosio, C. Turano, *Nucleic Acids Res.* 14 (1986) 5919.
- [10] R.F. Pasternack, E.J. Gibbs, J.J. Villafranca, *Biochemistry* 22 (1983) 5409.
- [11] L.G. Marzilli, *New J. Chem.* 14 (1990) 409, For review.
- [12] J.A. Strickland, L.G. Marzilli, W.D. Wilson, *Biopolymers* 29 (1990) 1307, For review.
- [13] B. Nordén, *Appl. Spectrosc. Rev.* 14 (1978) 157.
- [14] N.E. Geacintov, I. Victor, M. Rougee, R.V. Bensasson, *Biochemistry* 26 (1987) 3087.
- [15] U. Sehlstedt, S.K. Kim, P. Carter, J. Goodman, J.F. Volano, B. Nordén, J.C. Dabrowiak, *Biochemistry* 33 (1994) 417.
- [16] A. Wada, S. Kozawa, *J. Polym. Sci. A2* (1964) 853.
- [17] B. Nordén, F. Tjerneld, *Biophys. Chem.* 4 (1976) 191.
- [18] B. Nordén, S. Seth, *Appl. Spectrosc. Rev.* 39 (1985) 647.
- [19] B. Nordén, M. Kubista, T. Kurucsev, *Q. Rev. Biophys.* 25 (1992) 51.
- [20] B. Nordén, T. Kurucsev, *J. Mol. Recogni.* 7 (1994) 141.
- [21] B. Härd, B. Nordén, *Biopolymers* 25 (1986) 1209.
- [22] N.E. Mukundan, G. Pethö, D.W. Dixon, L.G. Marzilli, *Inorg. Chem.* 34 (1995) 3677.
- [23] J.B. Le Pecq, C. Paoletti, *J. Mol. Biol.* 29 (1967) 87.
- [24] M.A. Sari, J.P. Battioni, D. Dupré, D. Mansuy, J.B. Le Pecq, *Biochemistry* 29 (1990) 4205.
- [25] P.V. Scaria, R.H. Shafer, *J. Biol. Chem.* 266 (1991) 5417.
- [26] I. Haq, P. Linclon, D. Suh, B. Nordén, B.Z. Chowdhry, J.B. Chairs, *J. Am. Chem. Soc.* 117, p. 4788.
- [27] K.-M. Hyun, S.-D. Choi, S.K. Kim, *Biochim. Biophys. Acta* 1334 (1997) 312.
- [28] S. Eriksson, S.K. Kim, M. Kubista, B. Nordén, *Biochemistry* 32 (1993) 2987.
- [29] U. Sehlstedt, S.K. Kim, B. Nordén, *J. Am. Chem. Soc.* 115 (1993) 12258.
- [30] H.-K. Kim, J.-M. Kim, S.K. Kim, A. Rodger, B. Nordén, *Biochemistry* 35 (1996) 1187.
- [31] J.-H. Moon, S.K. Kim, U. Sehlstedt, A. Rodger, B. Nordén, *Biopolymers* 28 (1996) 593.